Non-oxidized graphene/elastomer composite films for wearable strain and pressure sensors with ultra-high flexibility and sensitivity

Meng, Q., Liu, Z., Cai, R., Lu, S. & Liu, T.

Original citation & hyperlink:
Meng, Q, Liu, Z, Cai, R, Lu, S & Liu, T 2020, 'Non-oxidized graphene/elastomer composite films for wearable strain and pressure sensors with ultra-high flexibility and sensitivity', Polymers for Advanced Technologies, vol. 31, no. 2, pp. 214-225.
https://dx.doi.org/10.1002/pat.4760

DOI 10.1002/pat.4760
ISSN 1042-7147
ESSN 1099-1581

Publisher: Wiley

Non-oxidized graphene/elastomer composite films for wearable strain and pressure sensors with ultra-high flexibility and sensitivity

Qingshi Meng [a], Zhiwen Liu[a], Rui Cai[b], Sensen Han[a], Shaowei Lu[c]*, Tianqing Liu[a, d]*

[a] College of Aerospace Engineering, Shenyang Aerospace University (SAU), Shenyang, 110136, China

[b] School of Mechanical, Aerospace and Automotive Engineering, Coventry University, Coventry, UK

[c] School of Materials Science and Engineering, Shenyang Aerospace University (SAU), Shenyang, 110136, China

[d] QIMR Berghofer Medical Research Institute, Brisbane Queensland, 4006, Australia

*Corresponding Authors: Shaowei Lu and Tianqing Liu
Emails: Lushaowei_2005@163.com; michelle.tianqing.liu@gmail.com

Abstract

It remains challenging to prepare wearable strain and pressure sensors with excellent mechanical properties, ultra-high flexibility and sensitivity. Electrically conductive graphene platelets (GnPs) with high structural integrity are used in making a composite film fabricated using robust fabrication techniques. The gauge factor for the strain is up to 100 at 0-5% strain and 50 at 5%-30% strain, and the sensitivity to pressure is 2.7×10^{-2} kPa^{-1} between 0-10 kPa and 1.5×10^{-4} kPa^{-1} between 300-1000 kPa. In addition, the flexible sensor demonstrates good repeatability and durability after 1000 cycles of tensile and compression tests. The flexible sensor has fast response ability and a wide operating temperature range, suggesting the excellent response to temperature. The flexible sensor is applied in monitoring several human motions as a wearable device with high accuracy. The ability to detect strain, pressure and temperature of the flexible sensor extends its applications to multifunctional wearable devices.

Key words: Graphene; Composite film; Strain and pressure sensor; Wearable device.

Running title: Graphene-based wearable strain and pressure sensors

1. Introduction

Stretchable and high sensitive sensors have attracted increasing interest with diverse applications including wearable devices [1-4], structural health monitoring systems [5] and artificial skin [6-8]. Flexible strain sensor and pressure sensor are mainly made of conductive composites consist of conductive filler and soft matrix [9-11]. Three main transduction mechanisms, including capacitance [12], piezoelectricity [13, 14], and piezoresistivity [15-17], depending on different composite materials, are identified for transduction of pressure or strain into electrical signals. Among the sensors with the above three transduction mechanisms, the piezoresistive sensor displays the superiorities of simple device structure, large measurement range and high sensitivity [18, 19]. However, most of the piezoresistive sensors are limited to only monitoring pressure or strain change [20-23]. Therefore, it is challenging to develop multifunctional flexible sensors with high sensitivity to both pressure and strain to enhance sensing versatility and reduce their cost in wearable devices.

The widely used matrix materials are the intrinsic elastic and extensible materials with high transparency and rapid respond to signals [24, 25], such as polyurethane (PU) [26], epoxy [27] and silicone rubber [28, 29]. These matrix materials provide the support for conductive fillers and determine the mechanical properties of composites. Considering flexibility and good fitness to the skin as a wearable device, silicone rubber has been selected as flexible substrate with advantages such as good elasticity and extensibility, rapid response to tensile and compression with skin-friendly breathability [30, 31].

The piezoresistance based flexible sensor mainly uses materials with excellent electrical conductivity as a filler to improve its electrical properties. Metal nanomaterials [32, 33] and carbon-based materials [5, 34, 35] are two types of the filler extensively studied. Amjadi et al. [36] prepared a flexible strain sensor with high sensitivity and good tensile properties by embedding silver nanowires film between two layers of polydimethylsiloxane (PDMS) in the form of sandwich structure. Its gauge factor reached up to 14, while the maximum tensile limit was up to 70%. Gong et al.[20] fabricated a wearable pressure sensor with ultra-thin gold nanowires and PDMS sheet, which detected low pressing forces with fast response, high sensitivity (more than 1.14 kPa^{-1}), and stability (more than 50,000 cycles). However, the precious metals lead to high fabrication cost. Additionally, the low compatibility with organic flexible substrates limited their applications. The discovery of

numerous conductive carbon-based materials such as carbon nanotube and graphene make it possible to solve this problem due to their advantages of light weight and good compatibility with organic materials. Yamada et al.[22] incorporated single-walled carbon nanotubes (SWCNTs) into a PDMS substrate by lamination. The prepared flexible strain sensor can achieve a large strain monitoring range (0-280%), which is 50 times higher than the traditional metal strain sensor. Wang et al.[37] prepared a flexible pressure sensor based on PDMS and SWCNTs, achieving superior sensitivity (1.80 kPa^{-1}), low detectable pressure limit (0.6 Pa), and fast response time (10 ms) for detection of feather-light pressures. However, SWCNTs have disadvantages of high cost and difficulties in industrial mass production. Multi-walled carbon nanotube (MWCNTs) is relatively cheaper with similar properties while the highly entangled structure makes them difficult for fabrication of composite thin-films. *Zhao et al. [38] fabricated a high-performance pressure sensor via constructing a unique conductive/insulating/conductive sandwich-like porous structure with ultra-sensitivity. Interpenetration of the conductive reduce graphene oxide network throughout the porous insulating interlayer produces a highly efficient transition from the non-conductive to the conductive state, the pressure sensor has a sensitivity of 0.67kPa^{-1} ($<$1.5kPa), fast response/recovery time ($\sim$10ms and $\sim$16 ms) and outstanding mechanical stability.*

More attention has been turned to graphene due to its excellent electrical conductivity (6000 S/cm) and exceptional mechanical properties (Young's modulus 1 TPa, tensile strength 130 GPa, stretch-ability 0~25%) [39-41]. However, independent of the chemical modification of graphene sheets, they have less electrical conductivity and less strength due to their relatively high defect concentration [42, 43]. These properties may cause negative effect on the performance of strain sensors [44].Graphene platelets (GnPs) [45-48] have been reported for fabrication of flexible sensors recently which have advantages, including large surface area for electron transfer, high electrical conductivity and cost effectiveness [27, 49]. *Therefore, high electrically conductive and structurally integrate GnPs instead of commonly used graphene oxide (GO) and RGO were selected for fabricating highly sensitive flexible sensor [50], which has great potential to detect strain and pressure. Each GnPs is 3 nm in thickness containing 1-4 layers of graphene sheets, offering sufficient interface to build conductive network, high C/O ratio (13.2) and high structural integrity resulting in high electrical conductivity of 1460 S/cm. In addition, the production cost for the sensor is low ($20/kg) [30, 35, 49].*

In this work, a composite material combining excellent mechanical properties of silicone rubber and great electrical properties of GnPs was fabricated by mixing the GnPs with silicone rubber. The preparation technique is simple, low-cost, scalable and robust. This composite material was used for the flexible sensor to detect temperature, strain and pressure with high sensitivity. To demonstrate the feasibility of the sensor applications, a range of wearable devices were fabricated to monitor human motions, including pulse movement, foot pressure and throat movement (mainly based on pressure signals) as well as finger bending, knee strain and cheek movement (mainly based on strain signals). Their performance was characterized and the promising results demonstrated that this flexible sensor has great potential to be as wearable devices and artificial skin.

2. Experimental section

2.1 Materials

The graphite intercalation compound (EG Asbury 1395) was kindly supplied by Asbury Carbons (NJ, USA). The silicone rubber (SYLGARD 184) was kindly supplied by Dow Corning (Zhangjiagang, China).

2.2 Fabrications of GnP/silicone rubber composite film

The GnPs were produced by a reported method [36, 37]. In brief, the graphite intercalation compound (Asbury 1395) was heated at 700°C for 1 min, and then sonicated for 2 h in acetone at 20°C. The prepared mixture was dried in the oven and the GnPs can be obtained.

Fig. 1 shows the fabrication process of GnP/silicone rubber composite film. The GnPs were dissolved in toluene and sonicated for 1h. The mixture was then added into the silicone solution, and the hardener was added thereafter at the ratio of 1:10 to silicone with stirring for 30 min. The obtained uniformly dispersed GnPs in mixtures were poured into the mold made of glass sheets and cured in an oven at 120^{o}C for 30 minutes. After curing process, the GnP/silicone rubber composite film was peeled from the mold. The composite film can be used as flexible sensor after wires are connected.

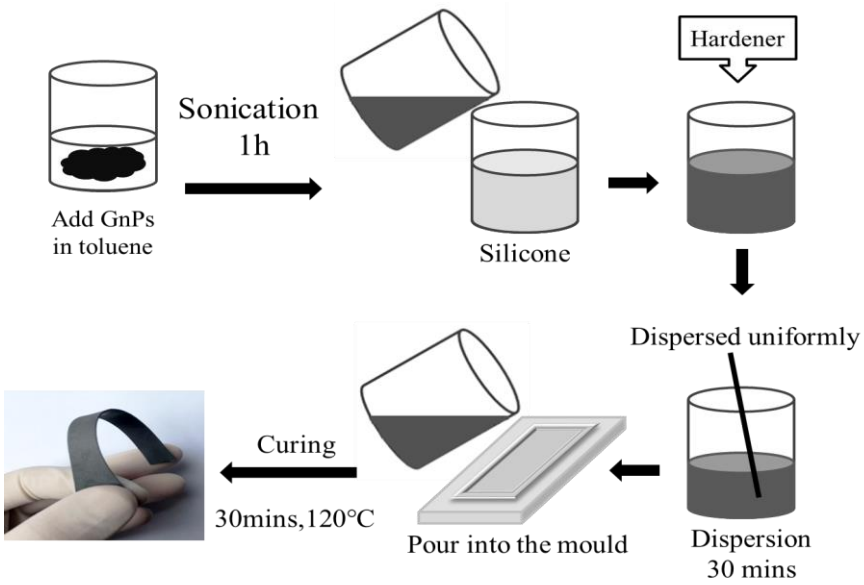

Fig. 1. the schematics of fabrication process of GnP/silicone rubber composite film.

2.3 Characterization of the performance of the sensor

Scanning electron microscope (SEM) was conducted using a SEM (JEOL JSM-7800F) with an accelerating voltage of 5 kV to show the composite films' cross section and surface. The high-magnification TEM images were taken from a JEOL microscope operated at 120kV. *1 vol% and 5 vol% composite films was also prepared scraped onto the 2 x 6 x 0.5 cm aluminum sheet with a piece of wood to form a transparent film about 0.25 cm thick for optical microscopic examination. We used an Olympus GX51 optical microscope to observe the imaging of a film at 1000 times magnification.*

The electrical conductivity of the films was measured with a high resistance meter (Agilent 4339B). Young's modulus (YM) and tensile strength (TS) were tested by tensile tests with a strain rate of 2 mm/min at room temperature of 20 °C. An Instron tensile machine was employed for the tensile testing in this project. Sensor property was based on the piezo-resistance theory and the electrical resistance (Changes) of the sensor was monitored using a FLUKE 2638A hydra series III data acquisition unit.

The strain sensitivity of the sensor is represented by the gauge factor, that is, the ratio of the changes in relative electrical resistance to the applied tensile strain. The gauge factor (GF) of the flexible sensor is calculated using the following equation [51, 52]:

$$GF = \frac{\Delta R/R_0}{\Delta L/L_0} \quad (1)$$

where R_0 is the initial resistance of the sensor, ΔR is the relative resistance change

under the deformation, L_0 is the initial length of the sensor, and ΔL is the relative elongation of the axial specimen. The gauge factor was collected by Instron tensile machine and FLUKE data acquisition unit to evaluate the relationship of the changes of electrical resistance and strain. The electrical resistance change was measured when dynamic strains were applied on the flexible sensor.

Similarly, the pressure sensitivity (S) is calculated using the following equation [9, 53]:

$$S = \frac{\delta(\frac{\Delta R}{R_0})}{\delta P} \quad (2)$$

Where R_o is the resistance of the sensor under standard atmospheric pressure (101.325kPa), ΔR is the relative resistance change under the loading pressure, P is the loading pressure on the sensor. FLUKE data acquisition unit was used to measure the resistance changes of the sensor under different static loading.

The repeatability testing was carried out to investigate the stability and durability of the sensor. The pressure of 100 kPa was applied 1000 cycles to the flexible sensor at the strain of 10% by an Instron tensile machine at a frequency of 1 Hz. The response time was monitored to study the responsiveness by measuring the time difference between loading and corresponding resistance changes, which could be calculated using the following equation:

$$t_s = T_o - T_i \quad (3)$$

Where t_s is the response time of flexible sensor applied signal s (strain or pressure), T_i is the time in which strain or pressure is applied, and T_o is the time in which the flexible sensor response to it.

The temperature response tests were carried out using the FLUKE data acquisition unit to record the resistance of flexible sensor under different temperature conditions. The program-controlled temperature furnace was used to control the temperature of the sensor from 30 to 100 ^oC. The hysteresis cycle tests were conducted to investigate the hysteresis performance of the flexible sensor. The phenomenon that the input/output characteristic curves do not coincide during the periods of input value increases from low to high (positive stroke) and the input value returns from high to low (reverse stroke) is hysteresis performance, which is used to values the error of the flexible for the stretch/release cycle.

The error could be calculated using the following equation:

$$E = |\Delta R_r - \Delta R_s| \quad (4)$$

Where E is the hysteresis error, ΔR_s is the output signal of applied strain ε during stretch, and ΔR_r is the output signal of the same applied strain ε during release.

The prepared flexible sensor was stuck on the surface of the test subject's skin to monitor the body health signals for the wearable applications. The FLUKE data acquisition unit was used to measure the resistance of the flexible sensor. The person with the sensor on is a healthy adult male with a body weight of about 80 kg.

3. Results and discussion

3.1 Characterization of GnP sheets

The morphology of GnP sheets was observed by TEM (Fig. 2a and 2b). The GnPs were observed on a copper TEM grid, clearly illustrating the flake-like structure. In general, the GnPs contain overlapped structures (indicated by black arrows in Fig. 2a). The relatively transparent and featureless area (red rectangle in Fig. 2a) likely possesses ultra-thin crystal structure (see enlarged image Fig. 2b). We randomly selected a point (indicated by red dash circle) to examine the electron diffraction (ED) pattern. Its ED pattern shows a typical six-fold symmetry expected for highly crystalline structure (right bottom). In addition, its diffraction illustrates a stronger outer ED than inner, confirming that the region contains few layers of graphene sheets [31, 32]. The high crystalline structure of the GnPs is in agreement with the XPS analysis (Fig. 2c), which shows a *C/O* ratio of 12.5:1.

In Fig. S1a (supporting information), the GnPs demonstrate obvious absorptions at 1340, 1585 and 2690 cm^{-1} which correspond to D, G, and 2D bands, respectively. G band refers to sp^2 resonance on an ordered graphitic lattice. D band is activated from the first-order scattering process of sp^2 carbons by the presence of in-plane substitutional hetero-atoms, vacancies, grain boundaries or other defects, which might be sp^3 hybridized carbon structure associating with the quantity of impurity or oxidation degree. Since all samples were tested in the form of powder, there is no point to discuss 2D band. The D- to G-band ratio of GnPs (I_D/I_G = 0.07) is much lower than those of reduced graphene oxide (~1 [54]) and GIC (0.57 [55]), revealing a far better structural integrity. This conclusion aligns with our TEM and XPS analysis. Fig. S1b (supporting information) contains FT-IR spectra of the GnPs. Our GnPs with high integrity contains sufficient functional groups for either chemical modification or promoting their dispersion in solvents.

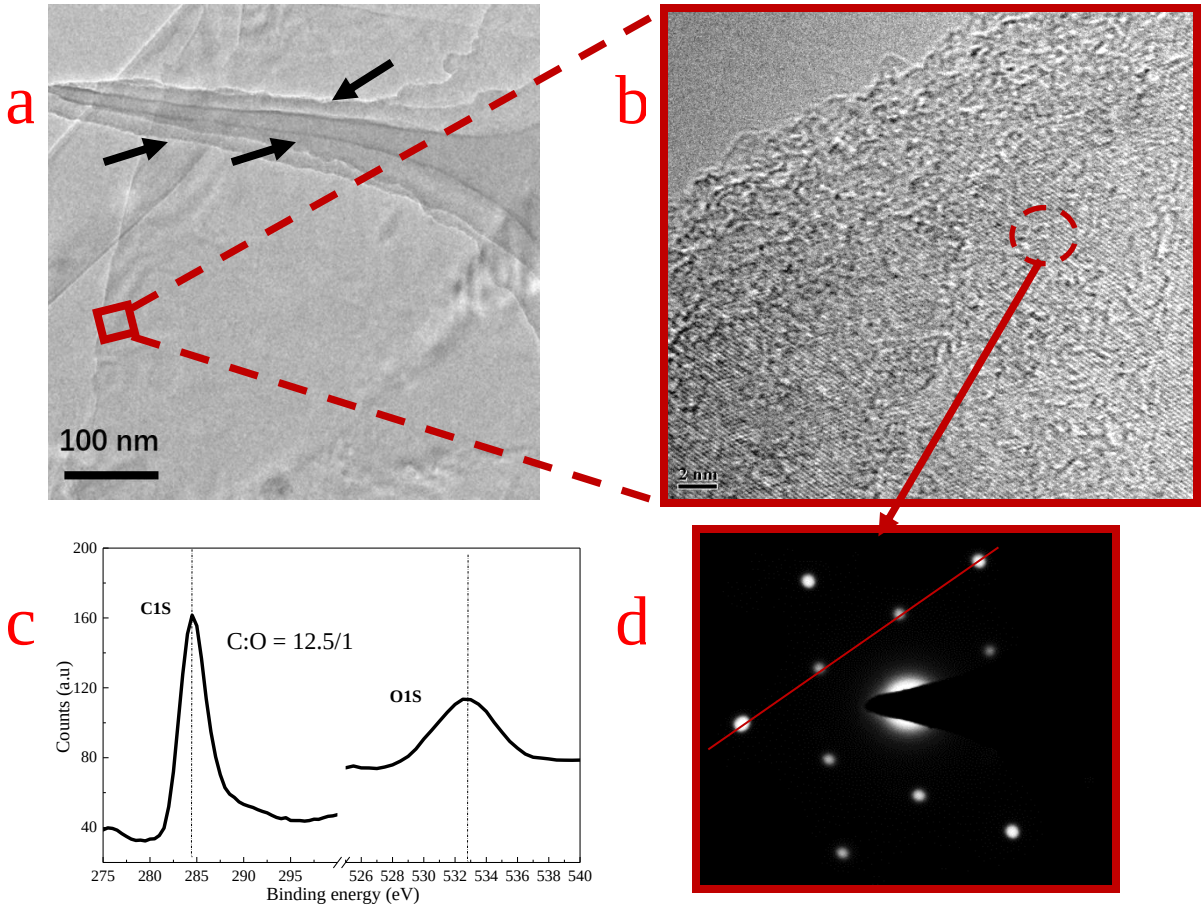

Fig. 2. The characterization of GnP sheets: (a) and (b) the TEM micrographs of a GnP sheet; and (c) the XPS of GnPs; andd) the electron diffraction (ED).

3.2 Morphology of GnP composite film

To investigate the microstructure of the GnP composite film, the SEM images of the GnP composite films with 1 vol% and 5 vol% of GnPs were compared in Fig. 3. The overall cross-sectional morphology of the GnP composite films demonstrates that the GnP sheets are well dispersed in silicone rubber, and different content of the GnP makes the dispersion density of the GnPs different (Fig. 3a and Fig. 3c). These structural changes may be responsible for the different electrical conductivity. Obviously, the higher the content of GnP in the composite film, the higher the number of conductive networks built, because the closely packed GnP sheets can form conductive paths. When the composite film is under strain or pressure, the extraneous force will make the composite extend or compress, resulting in the change of the conductive network inside of composite film. *In addition, the cross-sectional optical microscopy images of 1 vol% and 5 vol% composite films were shown in Fig. 3e and Fig. 3f, respectively. The dispersion of GnPs in the silicone rubber*

can be observed. The GnPs uniformly located within matrix and the dispersion density increased with GnPs content. This result is in agreement with the SEM results.

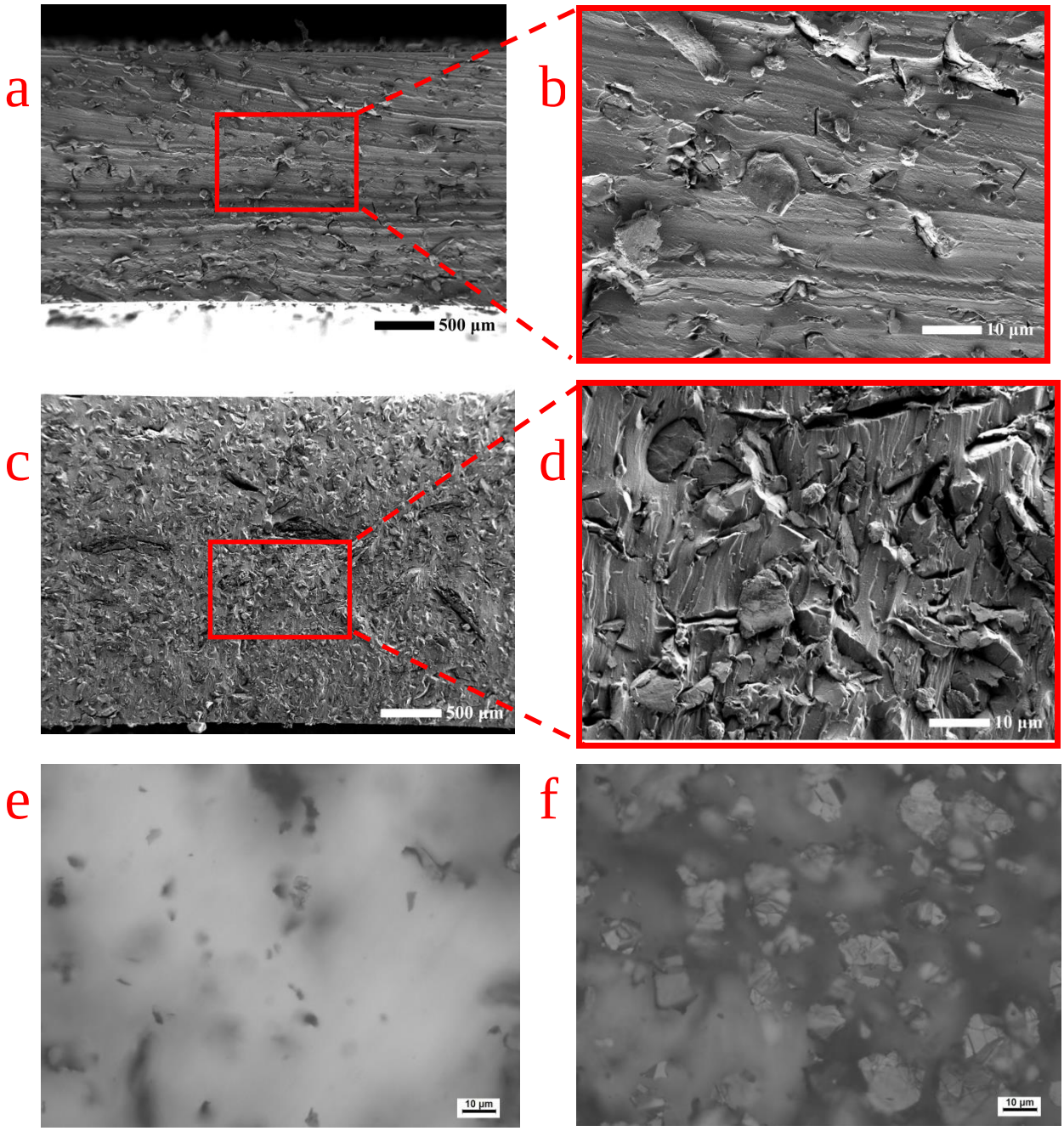

Fig. 3. The SEM and optical microscopy images of the GnP composite films with different contents: a) and (b) the cross-section SEM images of 1 vol% GnP composite film; (c) and (d) the cross-section SEM images of 5 vol% GnP composite film; and (e) and (f) the cross-section optical microscopy of 1 vol% and 5 vol% composite films.

3.3 Electrical conductivity

The electrical conductivity of GnP composite films with different contents were compared in Fig. 4. The electrical conductivity of GnP composite films increased with the content of

GnPs and a sharp rise appears at 2.5 vol% from 10^{-13} S/cm to 10^{-5} S/cm. By fitting experimental data into the power law equation, a percolation threshold (the formation of pathways for electron transfer) of 3.5 vol% GnPs and R^2 value of 97% was obtained, as shown in the inset of Fig. 4. *The percolation threshold is lower than previous works which means the composite materials have high conductivity at lower GnP content. This proves the excellent electrical conductivity of GnPs [56].*

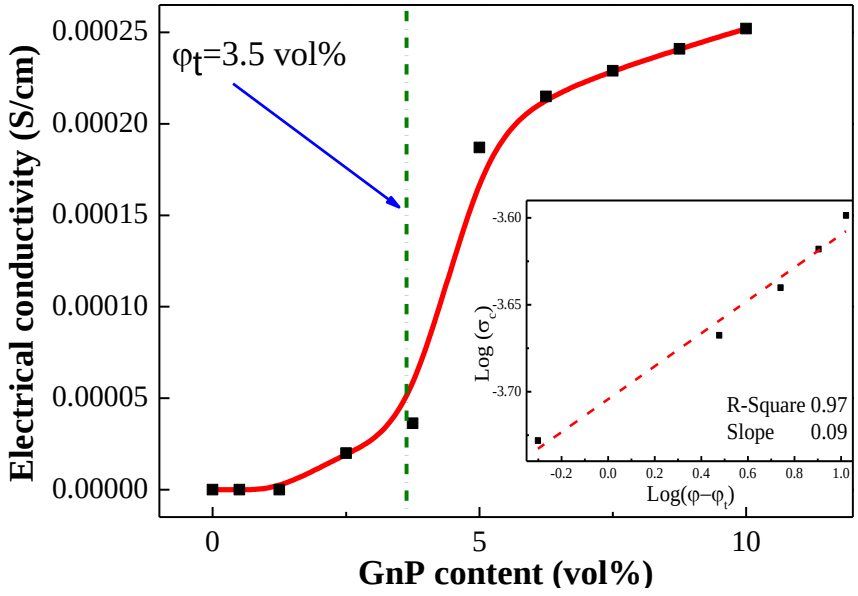

Fig. 4. The electrical conductivity of GnP composite films with different contents.

3.4 Mechanical property and flexible performance

The GnP composite film used as the flexible strain and pressure sensor needs to be strong enough to withstand large strains and pressures. To investigate the mechanical performance of the composite films, young's modulus and tensile strength was tested by Instron tensile machine. The Young's modulus of GnP composite films increases with GnP content, indicating the GnPs contribute to improve the Young's modulus of GnP composite films (Fig. 5a). On the contrary, the tensile strength decreases with the GnP content, mainly due to the sharp decrease of breaking elongation, as shown in Fig.5b. This result demonstrates that the composite films with high GnP content are easier to be stretched and compressed. The breaking elongation of composite film has a sharp decrease with GnP content, and thus the stretch ability of composite film decreases with GnP content. The Fig. 5c and Fig. 5d demonstrate the sensor could be bended and twisted with good electrical conductivity, indicating the excellent flexibility of the flexible sensor. Additionally, the resistance of the flexible sensor increases with the increasing of bending and twisting angles, which

indicates that the flexible sensor has the potential for angle detecting.

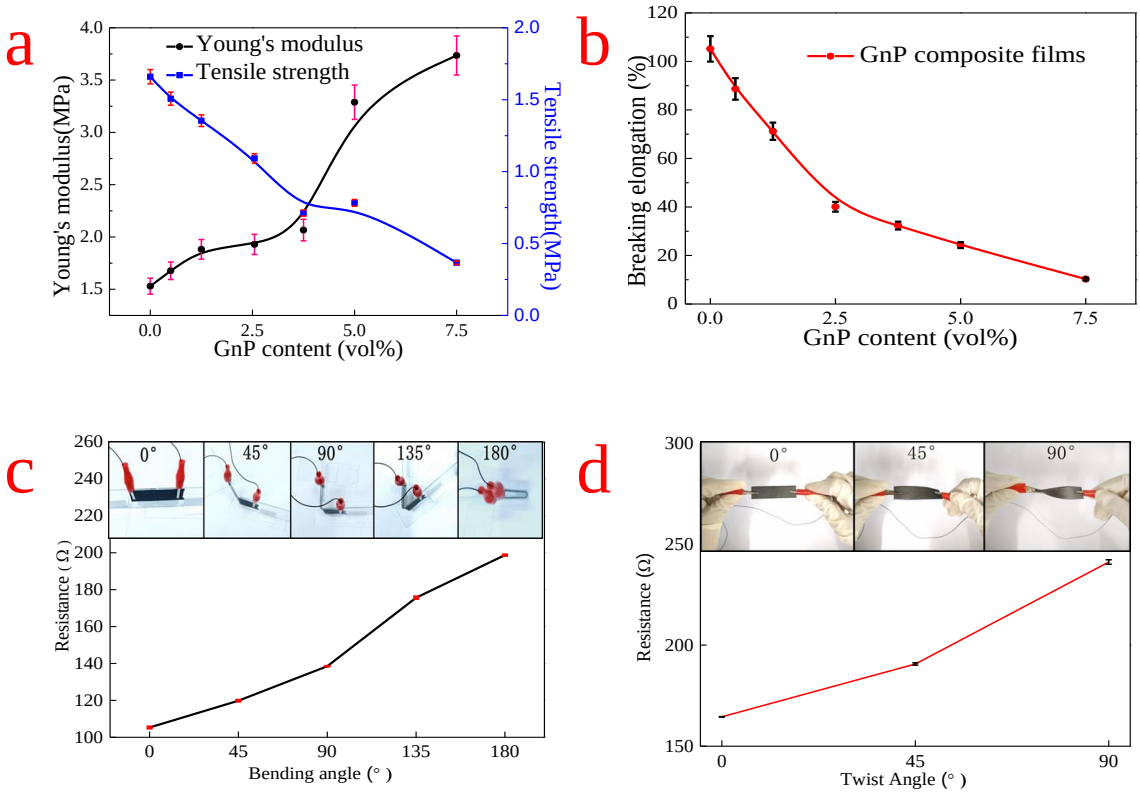

Fig. 5. The mechanical property of the GnP composite film: (a) the young's modulus and tensile strength of GnP composite films with different contents; (b) the breaking elongations of GnP composite films; (c) and (d) the flexibility testing of GnP composite film.

3.4 Sensitivity of flexible sensor

The flexible sensor was stretched by the tensile machine and its resistance change was measured by Fluke date acquisition unit to test its sensitivity to strain (Fig. 6a). *Fig. 6b demonstrates the mechanism of the resistance change of flexible sensor when strain is applied. The tensile force increases with the distance between adjacent graphene sheets, while decreases with the electrical conducting path, resulting in dramatic resistance change. The tensile force also stretches the length of the graphene sheets, causing further resistance change. Once the strain is unloaded, the structure of the GnP composite film recovers rapidly due to its elasticity, and the resistance restores simultaneously.* The ratio of electrical resistance change (ΔR) and the initial resistance (R_0) of the sensor were measured to show the response to the strain (Fig. 6c). There was an obvious increase with

the strain by comparing the electrical resistance of all composite films with different contents of GnPs. Among the four sensors, the one with 2.5 vol% GnPs shows the highest resistance change at the same strain range, and the widest strain measure range (0%-40%). The GF of the composite films was calculated and compared in Fig. 6d. The GF of small strain (0%-5%) is much higher than big strain, the 2.5 vol% GnP composite film shows highest GF which is up to 170 at 0-5% and 100 at 5%-40%, indicating the flexible sensor has better sensitivity to small strains. Although the trends of GF changes are consistent, the GF decreases with the GnP content in the composite films. In summary, the flexible sensor with 3.75 vol% GnP in composite film can achieve ideal electrical conductivity, mechanical performance and high strain sensitivity (high GF). Therefore, 3.75 vol% GnP in composite film was selected for the following experiments.

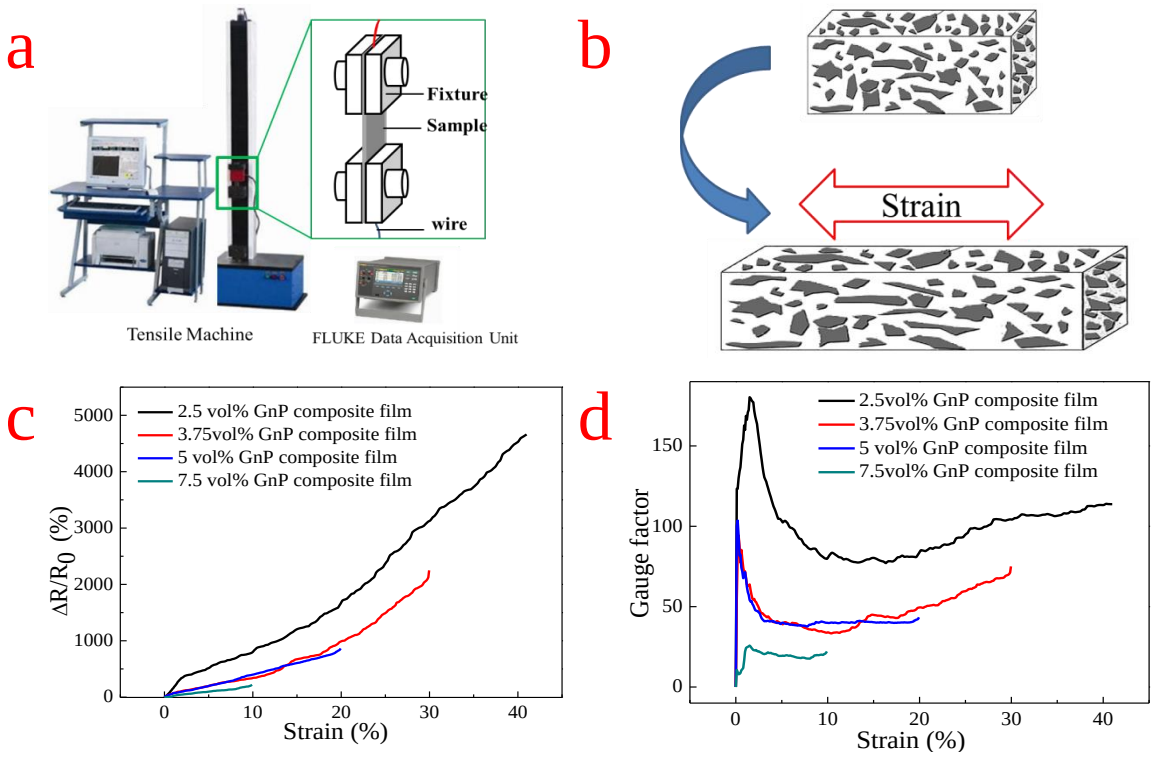

Fig. 6. The strain sensitivity testing of the flexible sensor: (a) the schematic of strain sensitivity testing, (b) the mechanism of the flexible sensor applied strain, (c) the curve of resistance changes and strain, and (d) the curves of gauge factor and strain.

The electrical resistance change was measured when different pressures were applied on the flexible sensor (Fig. 7a). *The distance between adjacent graphene sheets within the GnP composite film decreases under pressure, which results in the increase of conductive path, leading to a resistance change of flexible sensor.* Fig. 7b shows the resistance change

of the flexible sensor under different pressures. According to the result, the resistance decreases with pressure ranging up to 10 kPa. The decrease is particularly sharp with a high sensitivity of 2.7×10^{-2} kPa^{-1}. The sensitivity reaches 1.5×10^{-4} kPa^{-1} when the pressure ranging from 300 to 1000 kPa, demonstrating the flexible sensor has better sensitivity to pressure under smaller pressure values.

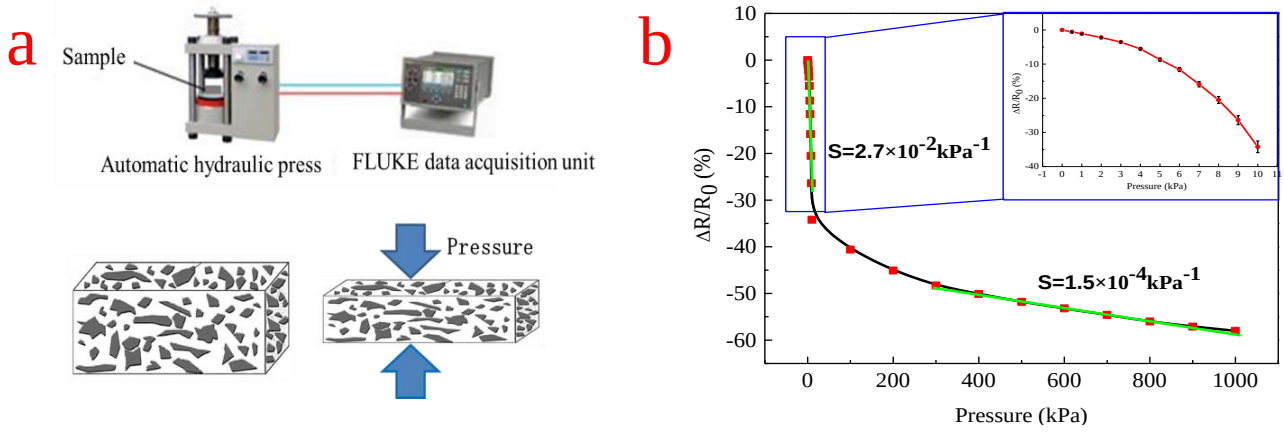

Fig. 7. The pressure sensitivity testing of the flexible sensor: (a) the schematic of pressure sensitivity and mechanism of flexible sensor applied pressure, and (b) the resistance changes of flexible sensor under different pressure and pressure sensitivity.

3.5 Repeatability and response time

We then conducted cyclic tensile and compress tests to study the stability and repeatability of the flexible sensor (Fig. 8a). The flexible sensor exhibits good stability after 1000 cycles at the strain of 10%, and the resistance change curves of first 10 times cycles and last 10 times cycles are in good repeatability. In Fig. 8b, the flexible sensor was compressed with pressure of 100 kPa in 1000 times cycles. The result demonstrates the flexible sensor has very good repeatability under pressure and the resistance change curve is very stable. The response time of the flexible sensor to strain and pressure is measured by the time interval between the time in which strain or pressure is applied and the time of in which the flexible sensor response to it [57]. The response time of the flexible sensor to strain of 10% is 50 ms, and the response time to pressure of 1 kPa is 89 ms, showing the flexible sensor responds to cyclic loading almost instantaneously, which proves it has quick response ability. In summary, this sensor has achieved high sensitivity with good stability and quick response ability.

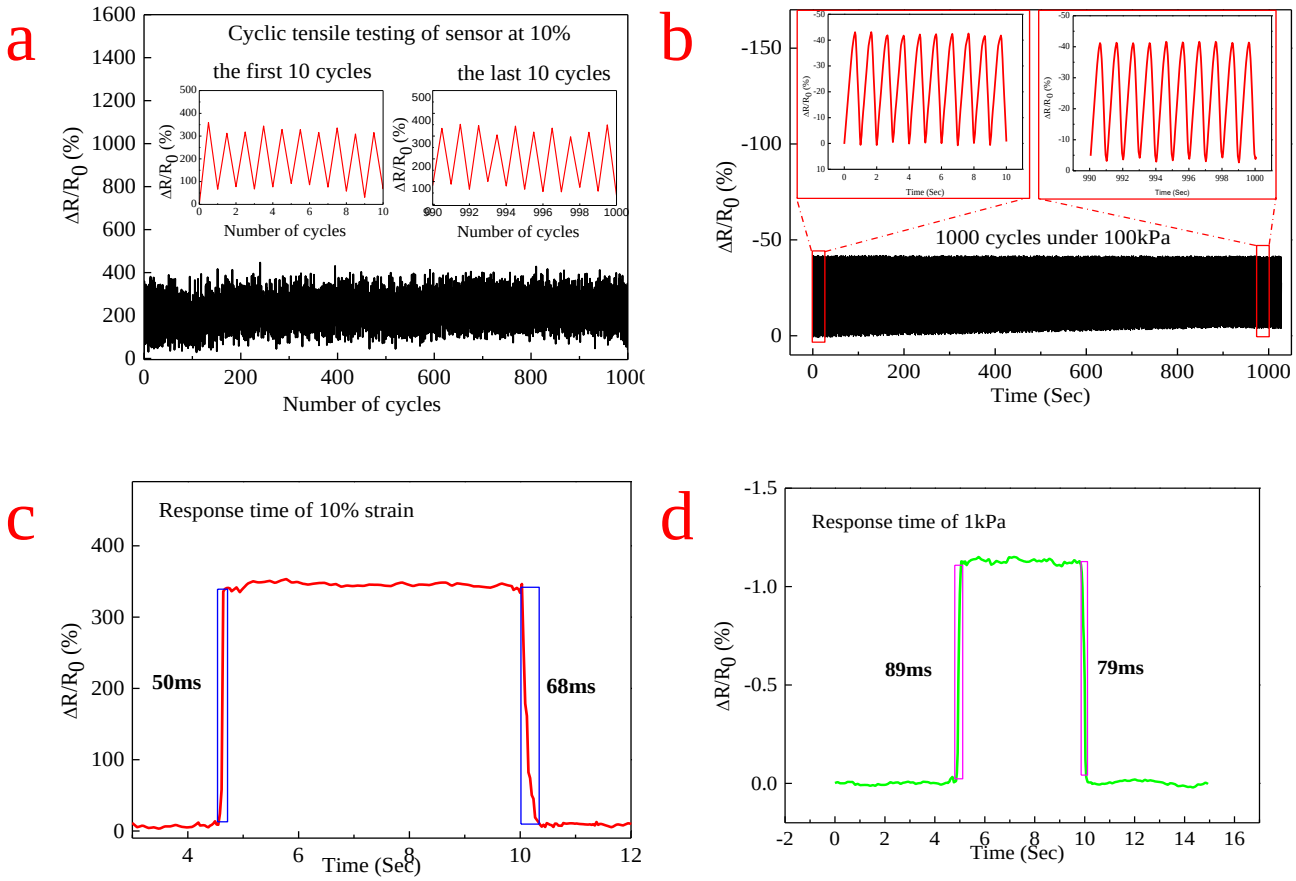

Fig. 8. Repeatability and response time testing: (a) The result of cyclic tensile testing of the sensor at 10%; (b) the result of cyclic compression testing under 100kPa; (c) the response time testing of 10% strain; and (d) the response time of 1kPa pressure.

3.6 Temperature response and hysteresis cycle

Electrical conductivity of most polymer composite materials may change with temperature, which is called temperature drift. The temperature response to flexible sensor was conducted over a temperature range of 20–100 ^{o}C (Fig. 9a). The resistance does not change significantly under 75 ^{o}C, while it increases sharply above 75 ^{o}C. According to the result, the strain sensor's appropriate operating temperature is 30-75 ^{o}C, temperature drift of the flexible sensor in this range is too tiny to consider. In addition, the resistance shows obvious response to temperature over 75 ^{o}C, this indicates that this flexile sensor has potential to be as a temperature sensor [58].

The cycle-strain hysteresis of the flexible sensor was measured to investigate the hysteresis performance (Fig. 9b). No obvious changes have been observed after applying 30% of strain loading compared with 30% of strain unloading, the hysteresis error is much less

than the resistance change during the stretch/release cycle Thus, the flexible sensor has good hysteresis performance according to the result.

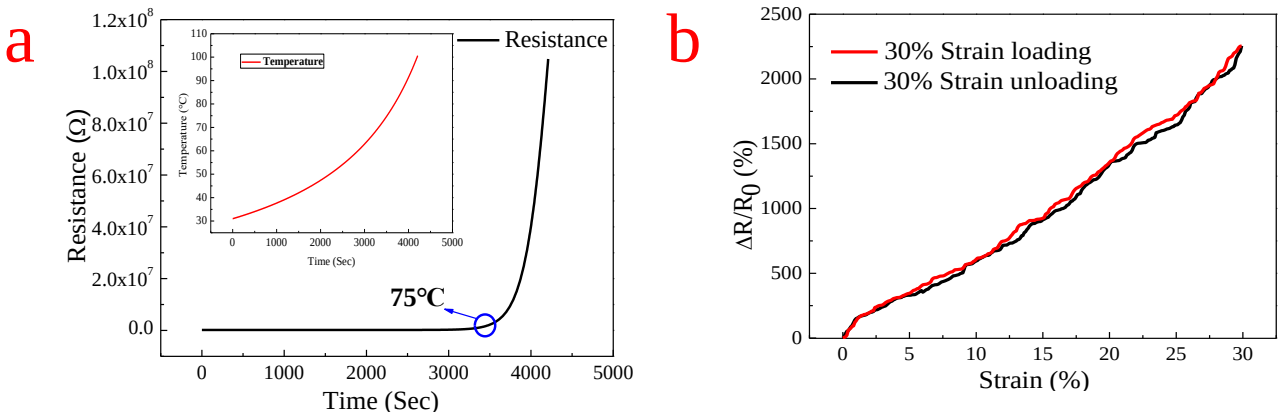

Fig. 9. (a) Temperature response of the flexible sensor, and (b) strain detecting hysteresis cycle of the flexible sensor.

3.7 Wearable application

The excellent flexibility, reliability, durability and sensitivity for both strain and pressure of our flexible sensors allowed their use as a wearable device for real-time monitoring human motions. Most human motions include both of pressure and strain signals together, while one of them may play the dominant role in one motion. In this work, pulse movement, foot pressure and throat movement mainly use pressure signals (blue rectangle), while finger bending, knee strain and cheek movement mainly use strain signal (red rectangle).

Fig. 10a is the result of the monitoring for cheek movement. The flexible sensor was attached on the face of a test subject to detect the strain of the skin when the test subject's mouth blew. The flexible sensor was stretched along with the cheek movement and recovered afterwards, resulting in the resistance change.

We then applied the flexible sensor to the throat to test the pressure changes at the throat during swallowing (Fig. 10b). In a swallowing operation, the movement of the larynx causes pressure change on the surface of the throat. The waveform of the resistance change caused by two swallowing actions is basically the same, the resistance decreases rapidly after the start of the swallowing action and returns to the original resistance after undergoing a twist, indicating that the flexible sensor can monitor the subtle human motion signal. This is important for the monitoring of subtle motion signals in wearable device applications.

The flexible sensor was attached tightly on a finger in a straight state to test the finger bending motion (Fig. 10c). The resistance of the sensor nearly remains constant with slight

fluctuation when the finger keeps straight. When the finger starts bending, the electrical resistance of the flexible sensor increases sharply, and the peak of the resistance change corresponds to the degree of finger bending motion. This result indicates the flexible sensor has the ability to detect the large-scale strain motion accurately.

The result of pulse movement monitoring is shown in Fig. 10d. The flexible sensor was attached on the wrist, the pulse movement of an adult male in the normal condition is around 12-13 beats per 10 seconds [59-61]. During the measurement, the flexible sensor was compressed and recovered when blood vessels dilate or constrict, resulting in the resistance change. According to the result, the flexible sensor monitors pulse movement accurately with details. The waveform is highly similar to the standard pulse movement waveform.

The pressure of the sole when walking is also monitored (Fig. 10e). Our results showed that the pressure of the sole is about 40 kPa when the test subject is standing and the resistance changes of the pressure sensor at the peak reflect the pressure of the standing state. When the foot is lifted, the pressure is instantly reduced back to the normal value. When walking at the speed of about 5 seconds per step, the peak value of the resistance changes according to the walking patterns, indicating that the sensor has an accurate and rapid response on monitoring the human motions. The foot pressure is the most effective means to monitor walking and running.

Finally, the sensor is attached to the knee meniscus to test the change of knee pressure during exercise. When the leg is in the straight state, the sensor resistance is basically stable. When the knee is bent, the meniscus at the knee is subjected to the pressure, which the sensor on the skin surface can detect, through rapidly changed resistance of the sensor. When the leg returns to the straight state, the sensor resistance recovers to its initial state. Since the knees are the key joints in human bodies, monitoring pressures in knee movements is essential in health check and exercise monitoring to avoid inappropriate use of the knees in normal life and exercises, which exerts unnecessary pressure on the knees.

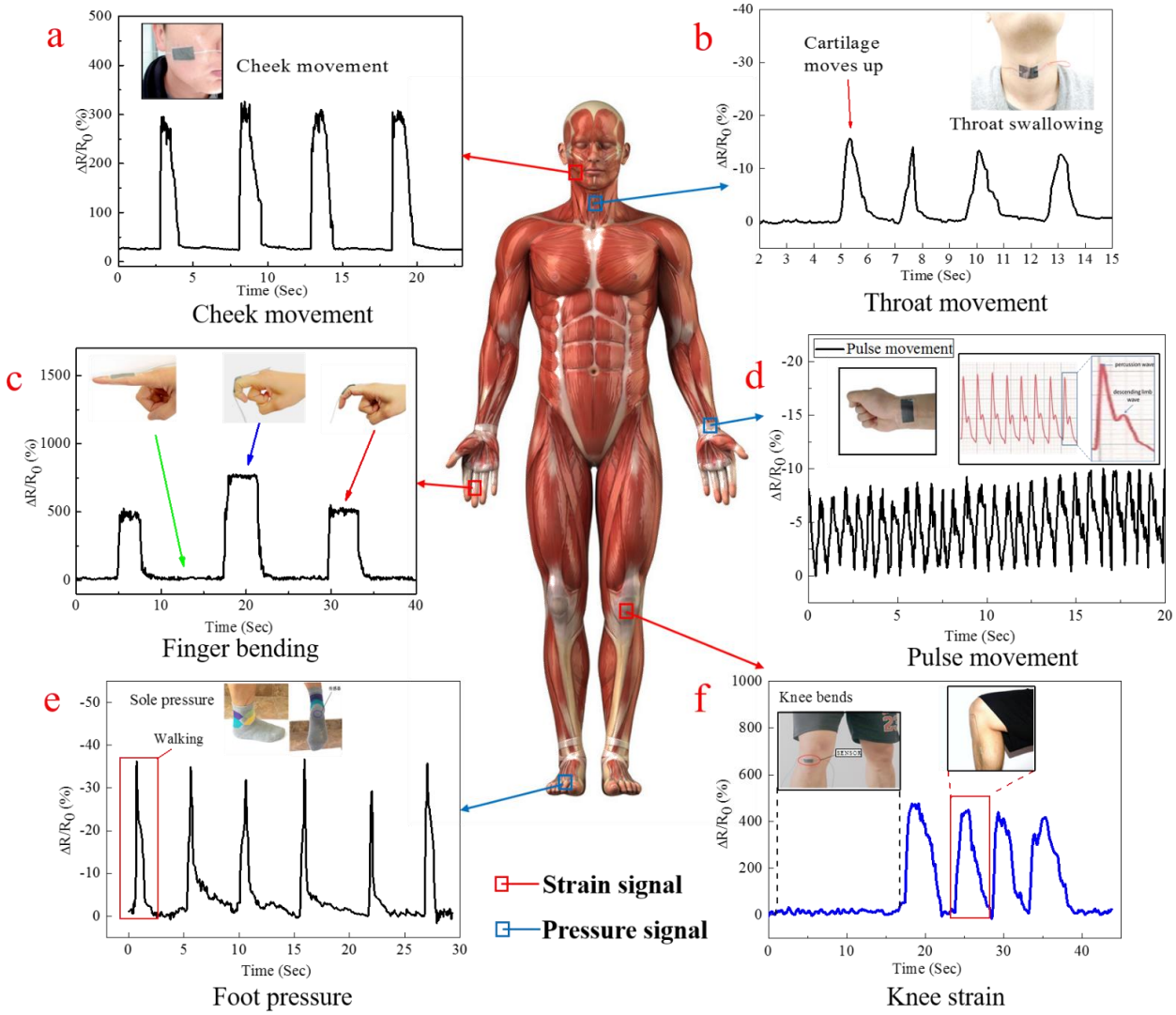

Fig. 10. Real-time monitoring of human motions using strain and pressure signals

According to the results, the flexible sensor developed in this work shows ideal performance in these testing, we made a comparison between the flexible sensor in this work and related works in order to show the advantages of this sensor. As shown in table 1, the flexible sensors were compared in terms of fabrication, sensitivity, range, response time and wearable ability. In contrast with the previously demonstrated flexible sensor, our flexible sensor exhibits various advantages, including: (1) facile and cost-effective approach to fabricate the sensor using solution processing method; (2) combining high sensitivity to strain and pressure, while other flexible sensors are only sensitive to one of strain and pressure or only the sensitivity to one signal is high and another is low; and (3) great potential in wearable device to detect different types of human motions and high

accuracy monitoring for several typical human motions.

Table 1. the comparison between the flexible sensors fabricated by different materials

Materials	*Fabrication*	*Sensitivity/ range*	*Response time*	*Wearable ability*	*Ref.*
GnPs/PET	*Spray coating*	*GF 150(0-2%)*	*N/A*	*×*	*[62]*
GnPs-PDMS foam	*Direct template*	*0.23kPa^{-1}(0-70kPa)*	*N/A*	*×*	*[24]*
AgNW-PDMS	*Micromolding*	*GF 2-14(0-70%)*	*N/A*	*✓*	*[36]*
PDMS/SWNTs	*Lamination*	*1.8 kPa^{-1}(0-1.2kPa)*	*10 ms*	*✓*	*[63]*
GPN/PDMS	*Coating*	*0.09 kPa^{-1} (0-3000 kPa) GF 8.5(0-40%)*	*100ms*	*✓*	*[9]*
GnPs/Silicone rubber	*Solution processing*	*0.027 kPa^{-1} (0-1000 kPa) GF 100 (0-30%)*	*50-90ms*	*✓*	*This work*

PET (Polyethylene terephthalate), AgNW (silver nanowire), SWNTs (signal wall nanotube), GPN (graphene porous network)

Conclusion

In conclusion， we reported that graphene/silicone rubber composites using the high structurally integrate and electrically conductive GnPs have achieved a good combination of mechanical and electrical properties. A flexible sensor made of composite film to detect strain and pressure was fabricated by a facial approach. The flexible sensor shows good sensitivity to both strain (100 at 0-5% strain and 50 at 5%-30% strain) and pressure (2.7×10^{-2} kPa^{-1} between 0-10 kPa and 1.5×10^{-4} kPa^{-1} between 300-1000 kPa). In addition, the flexible sensor has achieved good stability after more than 1000 cycles of strain and pressure, and quick response ability of 50 -80 ms. The flexible sensor was used to monitor real-time human's slight physiological signals and large-scale motions such as pulse movement and finger bending. The flexible sensor provides a promising platform for a wide range of applications with the advantages, including (i) simple fabrication and low cost, (ii) high structurally integrate and electrically conductive GnPs, (iii) sensitivity to strain and pressure, and (iv) accurately monitoring for multiple human motions.

Acknowledgments

QM would like to thank Asbury and Huntsman (Melbourne) for providing the graphite intercalation compounds (1395 and 1721). This work was financially supported by the Natural Science Foundation of Liaoning Province-China (20170520142), Aeronautical Science Foundation of China (2018ZF54036) and China Postdoctoral Science Foundation (2019M651151). Dr. Tianqing Liu is supported by NHMRC Early Career Fellowship (1112258).

Reference

[1] B.W. An, S. Heo, S. Ji, F. Bien, J.U. Park, Transparent and flexible fingerprint sensor array with multiplexed detection of tactile pressure and skin temperature, Nature Communications 9(1) (2018) 2458-.
[2] H. Ying, G. Le, Y. Zhao, X. Guo, C. Liu, L. Ping, Highly flexible fabric strain sensor based on graphene nanoplatelet–polyaniline nanocomposites for human gesture recognition, Journal of Applied Polymer Science 134(39) (2017) 45340.
[3] J. Yang, Y. Ye, X. Li, X. Lü, R. Chen, Flexible, conductive, and highly pressure-sensitive graphene-polyimide foam for pressure sensor application, Composites Science & Technology 164 (2018) 187-194.
[4] D. Tang, Q. Wang, Z. Wang, Q. Liu, B. Zhang, D. He, Z. Wu, S. Mu, Highly sensitive wearable sensor based on a flexible multi-layer graphene film antenna, Science Bulletin 63(9) (2018) 574-579.
[5] S. Lu, D. Chen, X. Wang, J. Shao, K. Ma, L. Zhang, S. Araby, Q. Meng, Real-time cure behaviour monitoring of polymer composites using a highly flexible and sensitive CNT buckypaper sensor, Composites Science and Technology 152 (2017) 181-189.
[6] C. Pang, G.Y. Lee, T.I. Kim, S.M. Kim, H.N. Kim, S.H. Ahn, K.Y. Suh, A flexible and highly sensitive strain-gauge sensor using reversible interlocking of nanofibres, Nature Materials 11(9) (2012) 795-801.
[7] Y. Ma, N. Liu, L. Li, X. Hu, Z. Zou, J. Wang, S. Luo, Y. Gao, A highly flexible and sensitive piezoresistive sensor based on MXene with greatly changed interlayer distances, Nature Communications 8(1) (2017) 1207.
[8] M. Ha, S. Lee, H. Ko, Wearable and flexible sensors for user-interactive health-monitoring devices, Journal of Materials Chemistry B 6(24) (2018).
[9] Y. Pang, H. Tian, L. Tao, Y. Li, X. Wang, N. Deng, Y. Yang, T.L. Ren, Flexible, highly sensitive, and wearable pressure and strain sensors with graphene porous network structure, ACS Appl Mater Interfaces 8(40) (2016) 26458–26462.
[10] Y. Liu, H. Wang, W. Zhao, M. Zhang, H. Qin, Y. Xie, Flexible, Stretchable Sensors for Wearable Health Monitoring: Sensing Mechanisms, Materials, Fabrication Strategies and Features, Sensors 18(2) (2018).
[11] Q. Meng, Y. Zhao, Z. Liu, S. Han, S. Lu, T. Liu, Flexible strain sensors based on epoxy/graphene composite film with long molecular weight curing agents, Journal of Applied Polymer Science 136(35) (2019) 47906.
[12] J. Ahn, J.W. Seo, T.I. Lee, D. Kwon, I. Park, T.S. Kim, J.Y. Lee, Extremely Robust and Patternable Electrodes for Copy-Paper-Based Electronics, ACS Appl Mater Interfaces

8(29) (2016) 19031-7.
[13] H. Kou, L. Zhang, Q. Tan, G. Liu, W. Lv, F. Lu, H. Dong, J. Xiong, Wireless flexible pressure sensor based on micro-patterned Graphene/PDMS composite, Sensors and Actuators A: Physical 277 (2018) 150-156.
[14] C. Dagdeviren, Y. Su, P. Joe, R. Yona, Y. Liu, Y.S. Kim, Y.A. Huang, A.R. Damadoran, J. Xia, L.W. Martin, Conformable amplified lead zirconate titanate sensors with enhanced piezoelectric response for cutaneous pressure monitoring, Nature Communications 5(7697) (2014) 4496.
[15] J. Shi, L. Wang, Z. Dai, L. Zhao, M. Du, H. Li, Y. Fang, Multiscale Hierarchical Design of a Flexible Piezoresistive Pressure Sensor with High Sensitivity and Wide Linearity Range, Small 14(27) (2018) e1800819.
[16] W. Huang, K. Dai, Y. Zhai, H. Liu, P. Zhan, J. Gao, G. Zheng, C. Liu, C. Shen, Flexible and lightweight pressure sensor based on carbon nanotube/thermoplastic polyurethane-aligned conductive foam with superior compressibility and stability, ACS Appl Mater Interfaces 9(48) (2017) 42266-42277.
[17] Q. Meng, Z. Liu, S. Han, L. Xu, S. Araby, R. Cai, Y. Zhao, S. Lu, T. Liu, A facile approach to fabricate highly sensitive, flexible strain sensor based on elastomeric/graphene platelet composite film, Journal of Materials Science 54(15) (2019) 10856-10870.
[18] B. Nie, X. Li, J. Shao, X. Li, H. Tian, D. Wang, Q. Zhang, B. Lu, Flexible and transparent strain sensors with embedded multiwalled carbon nanotubes meshes, ACS Appl Mater Interfaces 9(46) (2017) 40681-40689.
[19] B. Yin, Y. Wen, T. Hong, Z. Xie, G. Yuan, Q. Ji, H. Jia, Highly Stretchable, Ultrasensitive, and Wearable Strain Sensors Based on Facilely Prepared Reduced Graphene Oxide Woven Fabrics in an Ethanol Flame, ACS Appl Mater Interfaces 9(37) (2017) 32054-32064.
[20] S. Gong, W. Schwalb, Y. Wang, Y. Chen, Y. Tang, J. Si, B. Shirinzadeh, W. Cheng, A wearable and highly sensitive pressure sensor with ultrathin gold nanowires, Nature Communications 5(2) (2014) 3132.
[21] Y. Cheng, R. Wang, J. Sun, L. Gao, A Stretchable and Highly Sensitive Graphene-Based Fiber for Sensing Tensile Strain, Bending, and Torsion, Advanced Materials 27(45) (2016) 7365-7371.
[22] T. Yamada, Y. Hayamizu, Y. Yamamoto, Y. Yomogida, A. Izadi-Najafabadi, D.N. Futaba, K. Hata, A stretchable carbon nanotube strain sensor for human-motion detection, Nat Nanotechnol 6(5) (2011) 296-301.
[23] D.J. Lipomi, V. Michael, T. Benjamin C-K, S.L. Hellstrom, J.A. Lee, C.H. Fox, B. Zhenan, Skin-like pressure and strain sensors based on transparent elastic films of carbon nanotubes, Nature Nanotechnology 6(12) (2011) 788-792.
[24] A. Rinaldi, A. Tamburrano, M. Fortunato, M.S. Sarto, A Flexible and Highly Sensitive Pressure Sensor Based on a PDMS Foam Coated with Graphene Nanoplatelets, Sensors 16(12) (2016).
[25] G. Ge, Y. Cai, Q. Dong, Y. Zhang, J. Shao, W. Huang, X. Dong, A flexible pressure sensor based on rGO/polyaniline wrapped sponge with tunable sensitivity for human motion detection, Nanoscale 10(21) (2018) 10033-10040.
[26] J.F. Christ, N. Aliheidari, A. Ameli, P. Pötschke, 3D printed highly elastic strain sensors of multiwalled carbon nanotube/thermoplastic polyurethane nanocomposites, Materials & Design 131 (2017) 394-401.
[27] Q. Meng, H. Wu, Z. Zhao, S. Araby, S. Lu, J. Ma, Free-standing, flexible, electrically conductive epoxy/graphene composite films, Composites Part A: Applied Science and Manufacturing 92 (2017) 42-50.
[28] G. Li, K. Dai, M. Ren, Y. Wang, G. Zheng, C. Liu, C. Shen, Aligned flexible

conductive fibrous networks for highly sensitive, ultrastretchable and wearable strain sensors, Journal of Materials Chemistry C 6(24) (2018) 6575-6583.
[29] Z. Zhan, R. Lin, V.T. Tran, J. An, Y. Wei, H. Du, T. Tran, W. Lu, Paper/Carbon Nanotube-Based Wearable Pressure Sensor for Physiological Signal Acquisition and Soft Robotic Skin, ACS Appl Mater Interfaces 9(43) (2017) 37921-37928.
[30] G. Shi, Z. Zhao, J.-H. Pai, I. Lee, L. Zhang, C. Stevenson, K. Ishara, R. Zhang, H. Zhu, J. Ma, Highly Sensitive, Wearable, Durable Strain Sensors and Stretchable Conductors Using Graphene/Silicon Rubber Composites, Advanced Functional Materials 26(42) (2016) 7614-7625.
[31] Y. Liu, D. Zhang, K. Wang, Y. Liu, Y. Shang, A novel strain sensor based on graphene composite films with layered structure, Composites Part A: Applied Science and Manufacturing 80 (2016) 95-103.
[32] Z. Cao, R. Wang, T. He, F. Xu, J. Sun, Interface-Controlled Conductive Fibers for Wearable Strain Sensors and Stretchable Conducting Wires, ACS Appl Mater Interfaces 10(16) (2018) 14087-14096.
[33] S. Gong, W. Schwalb, Y. Wang, Y. Chen, Y. Tang, J. Si, B. Shirinzadeh, W. Cheng, A wearable and highly sensitive pressure sensor with ultrathin gold nanowires, Nat Commun 5 (2014) 3132.
[34] S. Araby, Q. Meng, L. Zhang, H. Kang, P. Majewski, Y. Tang, J. Ma, Electrically and thermally conductive elastomer/graphene nanocomposites by solution mixing, Polymer 55(1) (2014) 201-210.
[35] M.K. Filippidou, E. Tegou, V. Tsouti, S. Chatzandroulis, A flexible strain sensor made of graphene nanoplatelets/polydimethylsiloxane nanocomposite, Microelectronic Engineering 142 (2015) 7-11.
[36] M. Amjadi, A. Pichitpajongkit, S. Lee, S. Ryu, I. Park, Highly stretchable and sensitive strain sensor based on silver nanowire-elastomer nanocomposite, ACS Nano 8(5) (2014) 5154-63.
[37] W. Xuewen, G. Yang, X. Zuoping, C. Zheng, Z. Ting, Silk-molded flexible, ultrasensitive, and highly stable electronic skin for monitoring human physiological signals, Advanced Materials 26(9) (2014) 1336-1342.
[38] L. Zhao, F. Qiang, S.-W. Dai, S.-C. Shen, Y.-Z. Huang, N.-J. Huang, G.-D. Zhang, L.-Z. Guan, J.-F. Gao, Y.-H. Song, L.-C. Tang, Construction of sandwich-like porous structure of graphene-coated foam composites for ultrasensitive and flexible pressure sensors, Nanoscale 11(21) (2019) 10229-10238.
[39] K.S. Novoselov, A.K. Geim, S.V. Morozov, D. Jiang, M.I. Katsnelson, I.V. Grigorieva, S.V. Dubonos, A.A. Firsov, Two-dimensional gas of massless Dirac fermions in graphene, Nature 438(7065) (2005) 197-200.
[40] A.K. Geim, Graphene: status and prospects, Science 324(5934) (2009) 1530-4.
[41] S. Chun, Y. Choi, W. Park, All-graphene strain sensor on soft substrate, Carbon 116 (2017) 753-759.
[42] G. Shi, Q. Meng, Z. Zhao, H.C. Kuan, A. Michelmore, J. Ma, Facile Fabrication of Graphene Membranes with Readily Tunable Structures, ACS Appl Mater Interfaces 7(25) (2015) 13745-57.
[43] Q. Meng, H.-C. Kuan, S. Araby, N. Kawashima, N. Saber, C.H. Wang, J. Ma, Effect of interface modification on PMMA/graphene nanocomposites, Journal of Materials Science 49(17) (2014) 5838-5849.
[44] J. Ma, Q. Meng, I. Zaman, S. Zhu, A. Michelmore, N. Kawashima, C.H. Wang, H.C. Kuan, Development of polymer composites using modified, high-structural integrity graphene platelets, Composites Science & Technology 91(2) (2014) 82-90.
[45] I. Zaman, H.C. Kuan, J. Dai, N. Kawashima, A. Michelmore, A. Sovi, S. Dong, L.

Luong, J. Ma, From carbon nanotubes and silicate layers to graphene platelets for polymer nanocomposites, Nanoscale 4(15) (2012) 4578-86.
[46] I. Zaman, H.C. Kuan, Q. Meng, A. Michelmore, N. Kawashima, T. Pitt, L. Zhang, S. Gouda, L. Luong, J. Ma, A facile approach to chemically modified graphene and its polymer nanocomposites, Advanced Functional Materials 22(13) (2012) 2735-2743.
[47] M. Ezrin, Plastics Failure Guide: Causes and Prevention, Cincinnati, Ohio1996.
[48] S. Han, Q. Meng, S. Araby, T. Liu, M. Demiral, Mechanical and electrical properties of graphene and carbon nanotube reinforced epoxy adhesives: Experimental and numerical analysis, Composites Part A: Applied Science and Manufacturing 120 (2019) 116-126.
[49] M. Qingshi, J. Jian, W. Ruoyu, K. Hsu-Chiang, M. Jun, K. Nobuyuki, M. Andrew, Z. Shenmin, C.H. Wang, Processable 3-nm thick graphene platelets of high electrical conductivity and their epoxy composites, Nanotechnology 25(12) (2014) 125707.
[50] L.-Z. Guan, L. Zhao, Y.-J. Wan, L.-C. Tang, Three-dimensional graphene-based polymer nanocomposites: preparation, properties and applications, Nanoscale 10(31) (2018) 14788-14811.
[51] S. Zhang, H. Zhang, G. Yao, F. Liao, M. Gao, Z. Huang, K. Li, Y. Lin, Highly stretchable, sensitive, and flexible strain sensors based on silver nanoparticles/carbon nanotubes composites, Journal of Alloys and Compounds 652 (2015) 48-54.
[52] A. Nakamura, T. Hamanishi, S. Kawakami, M. Takeda, A piezo-resistive graphene strain sensor with a hollow cylindrical geometry, Materials Science and Engineering: B 219 (2017) 20-27.
[53] Y.H. Kwak, W. Kim, K.B. Park, K. Kim, S. Seo, Flexible heartbeat sensor for wearable device, Biosensors & bioelectronics 94 (2017) 250-255.
[54] J. Ma, **Q. Meng**, A. Michelmore, N. Kawashima, Z. Izzuddin, C. Bengtsson, H.-C. Kuan, Covalently bonded interfaces for polymer/graphene composites, Journal of Materials Chemistry A 1(13) (2013) 4255.
[55] I. Zaman, H.-C. Kuan, Q. Meng, A. Michelmore, N. Kawashima, T. Pitt, L. Zhang, S. Gouda, L. Luong, J. Ma, A Facile Approach to Chemically Modified Graphene and its Polymer Nanocomposites, Advanced Functional Materials 22(13) (2012) 2735-2743.
[56] C.-F. Cao, G.-D. Zhang, L. Zhao, L.-X. Gong, J.-F. Gao, J.-X. Jiang, L.-C. Tang, Y.-W. Mai, Design of mechanically stable, electrically conductive and highly hydrophobic three-dimensional graphene nanoribbon composites by modulating the interconnected network on polymer foam skeleton, Composites Science and Technology 171 (2019) 162-170.
[57] F. Qiang, S.-W. Dai, L. Zhao, L.-X. Gong, G.-D. Zhang, J.-X. Jiang, L.-C. Tang, An insulating second filler tuning porous conductive composites for highly sensitive and fast responsive organic vapor sensor, Sensors and Actuators B: Chemical 285 (2019) 254-263.
[58] H. Xu, Y. Li, N.-J. Huang, Z.-R. Yu, P.-H. Wang, Z.-H. Zhang, Q.-Q. Xia, L.-X. Gong, S.-N. Li, L. Zhao, G.-D. Zhang, L.-C. Tang, Temperature-triggered sensitive resistance transition of graphene oxide wide-ribbons wrapped sponge for fire ultrafast detecting and early warning, Journal of Hazardous Materials 363 (2019) 286-294.
[59] M.F. O'Rourke, A. Pauca, X.J. Jiang, Pulse wave analysis, Br J Clin Pharmacol 51(6) (2001) 507-22.
[60] I.B. Wilkinson, I.R. Hall, H. MacCallum, I.S. Mackenzie, C.M. McEniery, B.J. van der Arend, Y.E. Shu, L.S. MacKay, D.J. Webb, J.R. Cockcroft, Pulse-wave analysis: clinical evaluation of a noninvasive, widely applicable method for assessing endothelial function, Arteriosclerosis, thrombosis, and vascular biology 22(1) (2002) 147-52.
[61] T. Yang, X. Jiang, Y. Zhong, X. Zhao, S. Lin, J. Li, X. Li, J. Xu, Z. Li, H. Zhu, A Wearable and Highly Sensitive Graphene Strain Sensor for Precise Home-Based Pulse Wave Monitoring, ACS sensors 2(7) (2017) 967-974.

[62] M. Hempel, D. Nezich, J. Kong, M. Hofmann, A Novel Class of Strain Gauges Based on Layered Percolative Films of 2D Materials, Nano Letters 12(11) (2012) 5714-5718.
[63] X. Wang, Y. Gu, Z. Xiong, Z. Cui, T. Zhang, Silk-Molded Flexible, Ultrasensitive, and Highly Stable Electronic Skin for Monitoring Human Physiological Signals, Advanced Materials 26(9) (2014) 1336-1342.